Optica Applicata, Vol. XLI, No. 4, 2011

Acoustic frequency dependence of transmission characteristics in fiber acoustic gratings

HAO ZHANG, BO LIU*, JUNHAO TAO, HONGGUANG DONG, TIEYAN GUO, MENG ZHANG

Key Laboratory of Optical Information Science and Technology, Ministry of Education, Institute of Modern Optics, Nankai University, Tianjin 300071, P.R. China

*Corresponding author: liupipi@nankai.edu.cn

The dependence of transmission characteristics on acoustic frequency for an SMF-based acousto-optic tunable filter has been investigated in this paper. Experimental results indicate that multi-resonance peaks may turn up in the transmission spectrum when applied acoustic frequency is sufficiently high, and resonance wavelengths increase in proportion to the applied acoustic frequency for short resonance wavelength region, while they have opposite acoustic frequency responses for longer resonance wavelength region. Our numerical simulation proves that this phenomenon could be attributed to the non-monotonic phase matching curves of acoustic gratings, which would be helpful for the understanding of mode coupling mechanism in fiber acoustic gratings and design of fiber-based acousto-optic devices.

Keywords: acousto-optic tunable filter (AOTF), acousto-optic mode coupling, single-mode fiber (SMF), long period grating (LPG), acoustic grating.

1. Introduction

Since KIM *et al*. firstly reported an acousto-optic tunable filter (AOTF) based on single-mode fiber (SMF) in 1997 [1], AO interaction in optical fibers has attracted considerable research interest, and in recent years a good variety of fiber-optic devices, including gain flattening filter [2], acousto-optic switch [3], variable optical attenuator [4], polarization controller [5], *etc*., have been developed by applying flexural or torsional waves in bare optical fibers. In these devices, long period gratings (LPGs) could be normally produced owing to axial periodic refractive index perturbation induced by applied acoustic modulation, and therefore the mode coupling in acoustic gratings could be utilized for various purposes. As has been widely reported, dynamic reconfiguration of transmission spectrum could be realized by adjusting the frequency and intensity of applied acoustic wave to respectively control the resonance wavelength and transmission loss of a fiber-based AOTF. It should be noted that some of the previous related reports show that the resonance wavelength monotonically increases with applied acoustic frequency [6] while the others indicate

that there exists an inverse proportional relationship between the above two parameters [7–9]. However, the untypical acoustic frequency response behavior of resonance wavelength has not aroused sufficient notice, and as an important issue that affects the understanding and applications of AO effect in optical fibers, this phenomenon still needs to be further investigated.

In 2004, ZHI *et al*. theoretically analyzed the non-monotonic dependence of resonance wavelength on the grating period for photonic crystal fiber (PCF) based LPGs [10]. And in this paper, similar phenomenon was found to take place in fiber-based AOTFs. The filtering characteristics of an SMF-based AOTF were experimentally investigated for a wavelength range from 600 nm to 1700 nm. Experimental results indicate that the acoustic frequency response of resonance wavelength has non-monotonic relationships for different wavelength regions. Based on theoretical calculation of the phase matching relationship, we have shown that two resonance wavelengths originating from the mode coupling between LP_{01} core mode and the same higher order mode may simultaneously turn up for certain applied acoustic frequency. Further analysis proves that the non-monotonic dependence of grating period on resonance wavelength is the major factor that leads to the untypical frequency response behavior for different wavelength regions.

2. Experimental setup and mode coupling principle

Figure 1 shows a schematic diagram of our SMF-based AOTF test system. A PCF-based supercontinuum light source is employed to provide broadband input light covering a wavelength range of about 600 nm to 1700 nm. A segment of SMF with ~10 cm coating stripped is tightly stretched and then fixed by two fiber holders. To effectively apply acoustic wave onto the SMF, an aluminum (Al) horn is attached on the top surface of a round piezoelectric transducer (PZT) plate, and the tip of Al horn is pasted at one end of the bare fiber. Thus, when driven with a radiation frequency (RF) signal through a signal generator, the PZT produces an acoustic wave, which will be amplified and transmitted to the SMF via the Al horn. An optical spectrum analyzer is employed to monitor the transmission spectrum evolution of the AOTF as applied acoustic frequency changes.

When flexural acoustic wave is applied onto the SMF, the refractive index along fiber axis will be periodically perturbed, leading to the formation of an acoustic grating.

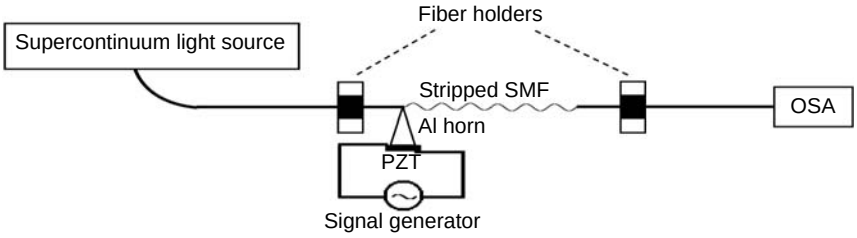

Fig. 1. Schematic diagram of the SMF-based AOTF test system.

As is well known, for LPGs the resonance wavelength originating from the mode coupling between core mode and certain cladding mode is determined by [11]:

$$\lambda_{\text{res}} = (n_{\text{co}} - n_{\text{cl}})\Lambda \tag{1}$$

where λ_{res} is resonance wavelength, n_{co} and n_{cl} represent effective refractive indexes of the fundamental core mode and certain cladding mode, respectively, and Λ represents grating period. Using the above equation, it is possible to acquire the dependence of grating period on resonance wavelength based on the effective refractive index difference between core mode and cladding mode when phase matching condition is maintained. Since the LPG is produced by flexural acoustic wave modulation, the grating period could be acquired by calculating the applied flexural mode acoustic period according to the following dispersion relation [12]:

$$\frac{\omega^2}{\beta^4} = \frac{a^2 E}{4\rho} \tag{2}$$

where ω and β are round frequency and propagation constant of flexural acoustic wave, respectively; E and ρ represent Young's modulus and density of rod-shaped acoustic medium, respectively; and a refers to rod radius. Considering $\omega = 2\pi f_a$ and $\beta = 2\pi/\lambda_a$, where f_a and λ_a are frequency and wavelength of applied acoustic wave, acoustic wavelength could be expressed in terms of frequency as:

$$\lambda_a = \left(\frac{\pi^2 a^2 E}{\rho f^2}\right)^{1/4} \tag{3}$$

As $\Lambda = \lambda_a$, by adjusting acoustic frequency, the resonance wavelength of AOTF will change accordingly. And by analyzing the phase matching curve based on acoustic period corresponding to experimental applied acoustic frequency range, we could acquire the information on mode coupling corresponding to the experimentally observed resonance peaks.

3. Experimental results and discussion

We have experimentally observed the evolution of transmission spectrum of the SMF-based AOTF as RF signal frequency changes. Throughout a wavelength range of 600–1700 nm, we found 4 resonance wavelength regions when the RF signal is driven around 3.2 MHz, 3.6 MHz, and 4.05 MHz, and the transmission spectra with largest transmission loss are shown in Figs. 2**a**–2**d**, respectively. As has been analyzed in Section 2, each of the resonance peaks originates from the mode coupling between fundamental core mode and certain higher mode. One interesting matter that should be addressed is that when acoustic frequency is adjusted to 4.05 MHz, two resonance wavelengths simultaneously turn up in the transmission spectrum. This indicates that the phase matching condition should be satisfied at these two wavelengths at the same time.

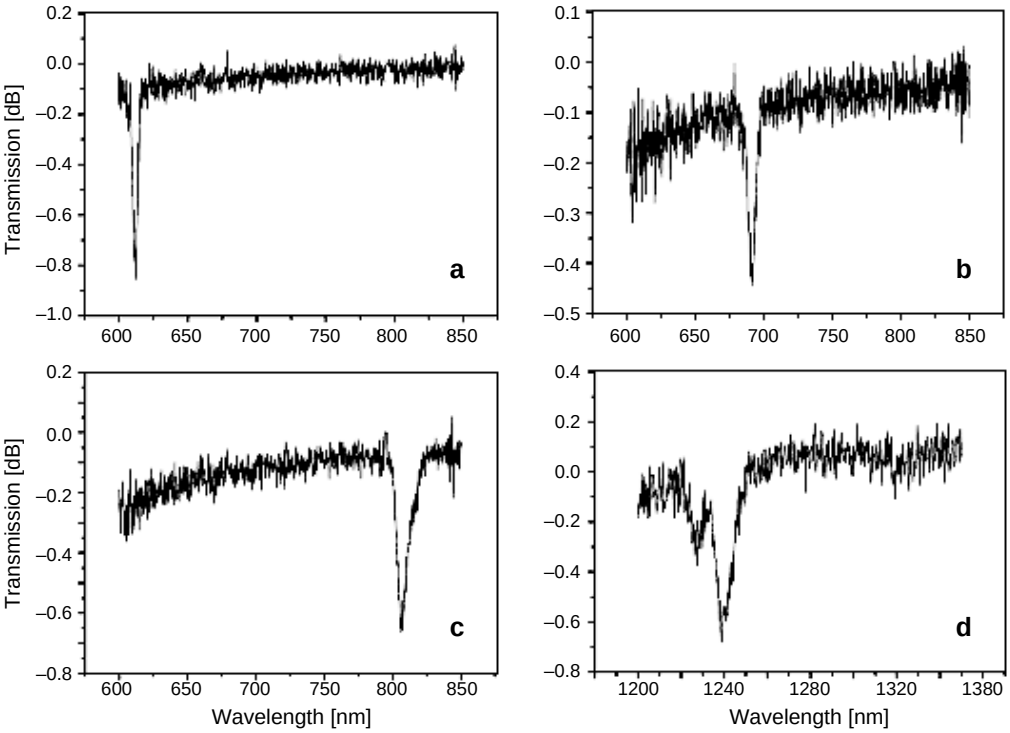

Fig. 2. Transmission spectra of the SMF-based AOTF as RF signal is driven at 3.2 MHz (region A) – **a**, 3.6 MHz (region B) – **b**, 4.05 MHz (region C) – **c**, and 4.05 MHz (region D) – **d**.

To analyze the mode coupling that may contribute to the formation of experimentally observed resonance peaks, we have calculated the dependence of grating period on resonance wavelength. According to typical parameters of SMF, such as Corning SMF-28 fiber (fiber radius: 62.5 μm; refractive index of the fiber core: 1.4681; refractive index difference: 0.36%), we could calculate the effective refractive index difference between LP_{01} mode and LP_{11} mode. And based on Eq. (1), grating period as a function of resonance wavelength for LP_{01}–LP_{11} mode coupling could be acquired, as depicted in Fig. 3. It is apparent that the grating period decreases as resonance wavelength increases from 575 nm to ~1160 nm, while it is proportional to resonance wavelength for higher wavelength region, *i.e.*, the grating period has a non-monotonic dependence on resonance wavelength. Based on Eq. (3) and considering E = 75.42 GPa and $\rho = 2.2\times10^3$ kg/m^3 for silica-based fibers, within an acoustic frequency range of 3.14 MHz to 4.1 MHz the period of acoustic grating is located between about 605 nm and 529.5 nm, corresponding to a resonance wavelength range of about 615 nm to 778 nm, which is basically in accordance with the experimental results in Figs. 2**a**–2**c**. It can also be seen that for 4.1 MHz RF signal another resonance region exists around 1480 nm, which corresponds to the resonance wavelength region in Fig. 2**d**. However, the inaccurate parameter settings adopted in our simulation cause some deviation from

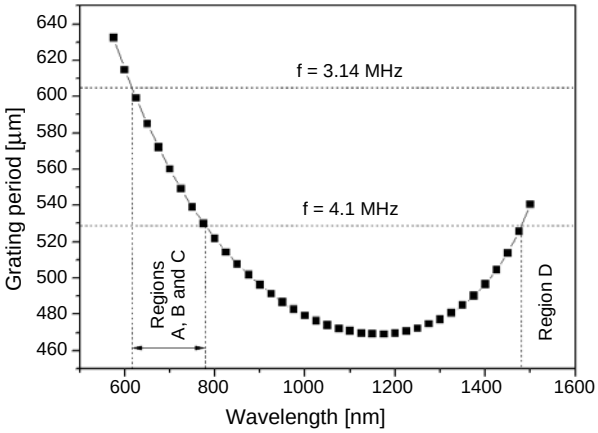

Fig. 3. Calculated grating period as a function of resonance wavelength for LP_{01}–LP_{11} mode coupling.

the experimental results. From Fig. 3, we can see that due to the non-monotonic dependence of grating period on resonance wavelength, two resonance wavelength regions may coexist when the RF signal frequency is high enough, which is in agreement with the experimental result in Figs. 2**c** and 2**d**.

To further confirm whether the mode coupling between LP_{01} core mode and other modes besides LP_{11} mode also contributes to the formation of resonance peaks, we have calculated the grating period as functions of resonance wavelength for mode coupling between LP_{01} mode and some low order modes, including LP_{21} mode, LP_{02} mode and LP_{31} mode, as illustrated in Fig. 4. It is clear that the grating periods corresponding to each of the three phase matching curves are below 300 nm. Considering that the acoustic grating period for our experiment is larger than about 530 nm, these 3 modes should not participate in the mode coupling process.

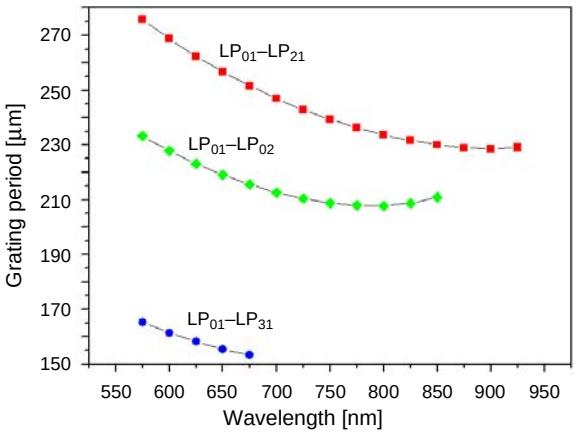

Fig. 4. Calculated grating period as functions of resonance wavelength for LP_{01}–LP_{21}, LP_{01}–LP_{02}, LP_{01}–LP_{31} mode couplings.

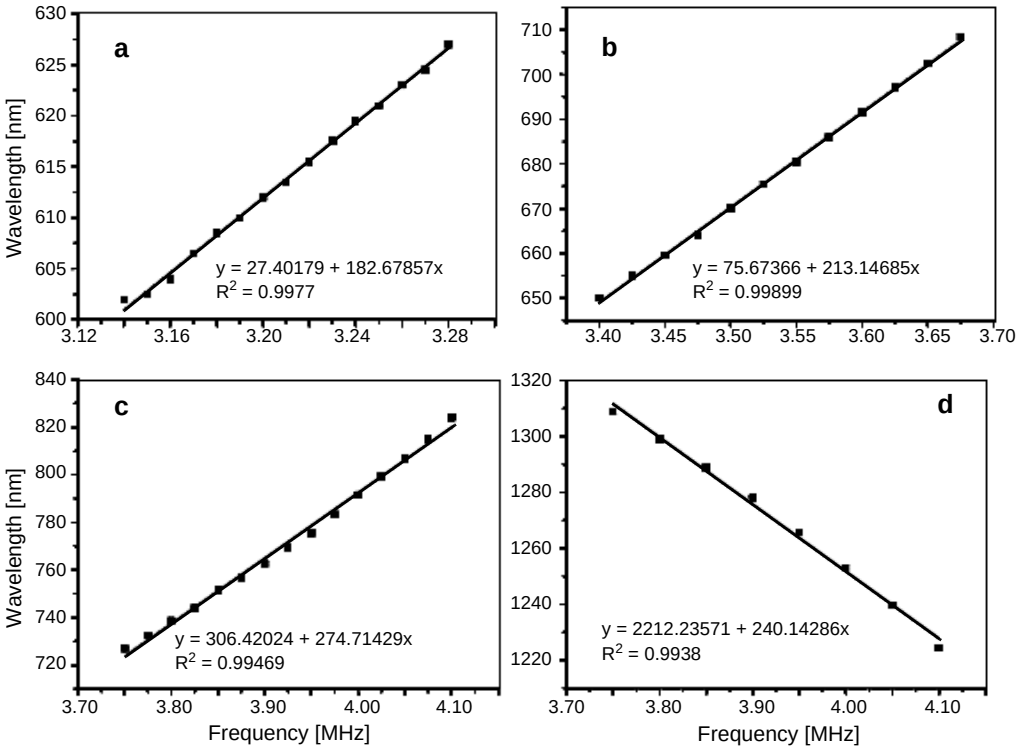

Fig. 5. RF signal frequency dependence of resonance wavelength for region A (**a**), region B (**b**), region C (**c**), and region D (**d**).

Figure 5 shows the resonance wavelength as functions of RF signal frequency for wavelength regions A–D, corresponding to those in Fig. 2. It can be seen that for the first three wavelength regions resonance wavelength linearly increases with the RF signal frequency while there exists an inverse proportion relationship between them for wavelength region D. The untypical frequency response behavior of resonance wavelength could be explained by the non-monotonic dependence of grating period on resonance wavelength as shown in Fig. 3. Since the acoustic wave period decreases with the increase of acoustic frequency, the dependence of resonance wavelength on acoustic grating period should present a trend inverse to the dependence of resonance wavelength on acoustic frequency. And therefore, the acoustic frequency response of resonance wavelength is different for wavelength regions beyond and below about 1160 nm.

4. Conclusions

In summary, we have investigated the dependence of transmission characteristics of an SMF-based AOTF on applied acoustic frequency. Experimental results show that multi-resonance may be excited when RF signal frequency is high enough and

the resonance peaks may have different acoustic frequency response behavior for different wavelength regions. Theoretical simulation indicates that the resonance wavelength dependence of grating period is non-monotonic, which leads to the untypical acoustic frequency responses of resonance peaks for the wavelength regions located on both sides of the yielding point of the phase matching curve. The work presented in this paper would be helpful for proper understanding of the unusual transmission properties of acoustic gratings, which is of fair importance to related research and applications of fiber-based AOTF devices.

Acknowledgements – This work was jointly supported by the National Natural Science Foundation of China under Grant Nos. 11004110 and 10904075, the Fundamental Research Funds for the Central Universities, the Science and Technology Support Project of Tianjin under Grant No. 11ZCKFGX01800, the National Key Basic Research and Development Program of China under Grant No. 2010CB327605, and the "100 Projects" of Creative Research for the Undergraduates of Nankai University under Grant No. BX8-142.

References

[1] KIM H.S., YUN S.H., KWANG I.K., KIM B.Y., *All-fiber acousto-optic tunable notch filter with electronically controllable spectral profile*, Optics Letters **22**(19), 1997, pp. 1476–1478.

[2] KIM H.S., YUN S.H., KIM H.K., PARK N., KIM B.Y., *Actively gain-flattened erbium-doped fiber amplifier over 35nm by using all-fiber acoustooptic tunable filters*, IEEE Photonics Technology Letters **10**(6), 1998, pp. 790–792.

[3] PARK H.S., SONG K.Y., YUN S.H., KIM B.Y., *All-fiber wavelength-tunable acoustooptic switches based on intermodal coupling in fibers*, Journal of Lightwave Technology **20**(10), 2002, pp. 1864–1868.

[4] LI Q., AU A.A., LIN C., LYONS E.R., LEE H.P., *An efficient all-fiber variable optical attenuator via acoustooptic mode coupling*, IEEE Photonics Technology Letters **14**(11), 2002, pp. 1563–1565.

[5] DASHTI P.Z., LI Q., LEE H.P., *All-fiber narrowband polarization controller based on coherent acousto-optic mode coupling in single-mode fiber*, Optics Letters **29**(20), 2004, pp. 2426–2428.

[6] DIMMICK T.E., KAKARANTZAS G., BIRKS T.A., DIEZ A., RUSSEL P.S.J., *Compact all-fiber acoustooptic tunable filters with small bandwidth-length product*, IEEE Photonics Technology Letters **12**(9), 2000, pp. 1210–1212.

[7] LEE K.J., PARK H.C., PARK H.S., KIM B.Y., *Highly efficient all-fiber tunable polarization filter using torsional acoustic wave*, Optics Express **15**(19), 2007, pp. 12362–12367.

[8] LEE K.J., YEOM D.I., KIM B.Y., *Narrowband, polarization insensitive all-fiber acousto-optic tunable bandpass filter*, Optics Express **15**(6), 2007, pp. 2987–2992.

[9] LEE K.J., HWANG I., PARK H.C., KIM B.Y., *Sidelobe suppression in all-fiber acousto-optic tunable filter using torsional acoustic wave*, Optics Express **18**(12), 2010, pp. 12059–12064.

[10] ZHI W., JIAN J., JIN W., CHIANG K.S., *Scaling property and multi-resonance of PCF-based long period gratings*, Optics Express **12**(25), 2004, pp. 6252–6257.

[11] ERDOGAN T., *Fiber grating spectra*, Journal of Lightwave Technology **15**(8), 1997, pp. 1277–1294.

[12] THURSTON R.N., *Elastic waves in rods and clad rods*, Journal of Acoustical Society of America **64**(1), 1978, pp. 1–37.

Received March 17, 2011
in revised form April 4, 2011